Check for updates

Chemical profiles with cardioprotective and anti-depressive effects of *Morus macroura* Miq. leaves and stem branches dichloromethane fractions on isoprenaline induced post-MI depression†

Dalia I. Hamdan,[a] Samia S. Hafez,[b] Wafaa H. B. Hassan,[b] Mai M. Morsi,[b] Heba M. A. Khalil, [ID] *[c] Yasmine H. Ahmed,[d] Omar A. Ahmed-Farid[e] and Riham A. El-Shiekh [ID] *[f]

This study was conducted to explore the potential cardioprotective and anti-depressive effects of dichloromethane (DCM) fractions of *Morus macroura* leaves (L) and stem branches (S) on post-myocardial infarction (MI) depression induced by isoprenaline (ISO) in rats in relation to their metabolites. The study was propped with a UPLC-ESI-MS/MS profiling and chromatographic isolation of the secondary metabolites. Column chromatography revealed the isolation of lupeol palmitate (**6**) that was isolated for the first time from nature with eight known compounds. In addition, more than forty metabolites belonging, mainly to flavonoids, and anthocyanins groups were identified. The rats were injected with ISO (85 mg kg^{-1}, s.c) in the first two days, followed by the administration of *M. macroura* DCM-L and DCM-S fractions (200 mg kg^{-1} p.o) for 19 days. Compared with the ISO exposed rats, the treated rats displayed a reduction in cardiac biomarkers (LDH and CKMB), anxiety, and depressive-like behaviour associated with an increase in the brain defense system (SOD and GSH), neuronal cell energy, GABA, serotonin, and dopamine, confirmed by histopathological investigations. In conclusion, DCM-L and DCM-S fractions' cardioprotective and anti-depressive activities are attributed to their metabolite profile. Therefore, they could serve as a potential agent in amending post-MI depression.

1. Introduction

Myocardial infarction (MI) is a severe health illness affecting approximately 600 individuals per 100 000 people.[1–3] Of the sequelae of MI is the depression that leads to high morbidities and mortalities globally.[2] The relation between the heart and brain in the pathogenesis of depression associated with MI (post-MI depression) remains unclear.[3] However, several medications have been used to treat either MI or depression but with no dual effect on the whole disease. Also, these medications have a high cost that leads to the discontinuation of the treatment protocol. Therefore, it is essential to investigate new medicines that have a dual effect on post-MI depression associated with studying possible mechanisms underlying this condition. Several traditional approaches have been adopted to use medicinal plants with various bioactive compounds to treat several diseases.

Morus, commonly known as mulberries, is an economically and medically important genus in Moraceae. It has valuable bioactive compounds that showed many potential activities such as antidiabetic, hepatoprotective, antibacterial, anti-inflammatory, antihypertensive, antiarthritic, antiviral, and antioxidative.[4]

Among the plant species, *M. macroura* possesses many beneficial compounds with therapeutic activities. It includes phenolic compounds (stilbene and stilbene dimers, prenylated and ger-anylated flavanones, 2- arylbenzofurans), a variety of Diels–Alder adducts (prenylated benzaldehyde-chalcone, prenylated chal-cone–chalcone, prenylated 2-arylbenzofuranchalcone, and pre-nylated stilbene-chalcone), and triterpenes.[5]

Therefore, the current study includes UPLC-ESI-MS/MS profiling and chromatographic isolation of the secondary

[a]*Department of Pharmacognosy and Natural Products, Faculty of Pharmacy, Menoufia University, Shibin Elkom, 32511, Egypt*

[b]*Pharmacognosy Department, Faculty of Pharmacy, Zagazig University, Zagazig 44519, Egypt*

[c]*Department of Veterinary Hygiene and Management, Faculty of Veterinary Medicine, Cairo University, Giza, 12211, Egypt. E-mail: heba.ali315@gmail.com; Tel: +201013666331*

[d]*Department of Cytology and Histology, Faculty of Veterinary Medicine, Cairo University, Giza, 12211, Egypt*

[e]*Department of Physiology, National Organization for Drug Control and Research, Giza, Egypt*

[f]*Department of Pharmacognosy, Faculty of Pharmacy, Cairo University, Kasr El Aini St., Cairo, 11562, Egypt. E-mail: riham.adel@pharma.cu.edu.eg; Tel: +201064763764*

† Electronic supplementary information (ESI) available. See DOI: 10.1039/d1ra08320a

metabolites using column chromatography for dichloromethane fraction of leaves (DCM-L) and dichloromethane fraction of stems (DCM-S) of *M. macroura*, then the evaluation of these fractions against post-MI depression induced by isoprenaline (ISO) in rats. Also, we assessed many underlying parameters, including depressive-like behavior, biochemical, and histopathological profile. It is worth noting that ISO is a widely used inducer for MI at high doses in preclinical studies and showed many metabolic and morphologic aberrations in experimental animals.[6,7] Many studies induce post-MI depression surgically.[8,9] However, in our study, we depend on a non-invasive method in the induction using ISO based on previous research,[10] which demonstrates depressive-like behaviour and myocardial injury after administration of isopropyl adrenaline.

2. Material and methods

2.1. Plant material

Leaves and stem branches were collected from *M. macroura* Miq. tree cultivated on the farm of the Department of Pharmacognosy, Faculty of Pharmacy, Zagazig University 2020. A voucher specimen (MM100) kept at the department's herbarium was kindly identified by Prof. Dr Abdelhalem Abdelmogali, Taxonomy researcher, Ministry of Agriculture, Dokki- Cairo (Egypt). The leaves and stem branches of the plant under investigation were air-dried, ground separately into fine powders, and kept in a well-closed container until use.

2.2. Extraction, fractionation, and chromatographic isolation of secondary metabolites

Air-dried powdered leaves (1.5 kg) and stem branches (2 kg) of *M. macroura* were separately extracted with 80% aqueous ethanol at room temperature. The ethanol extracts (leaves 350.0 g) and (stem branches 135.0 g) were subsequently partitioned against DCM and ethyl acetate. DCM fractions of the leaves and stems were 65.0 and 30.0 g, respectively.

Thin layer chromatography (TLC) fingerprinting of DCM fractions obtained from leaves and stem branches revealed almost the same profiling; thus, a mixture of 40 g from the two fractions was mixed with 40 g of silica gel for the column to get a dry mixed initial zone, which was applied on the top of the silica gel column (6 × 150 cm, 800 g) packed using the wet method with *n*-hexane. The polarity was increased gradually using DCM then methanol and fractions (250 mL each) were collected, concentrated under reduced pressure, examined by TLC, and similar fractions were combined. Besides this, column fractions (9–13) eluted using 5% CH_2Cl_2/*n*-hexane revealed the presence of one major blue spot (using anisaldehyde–sulphuric) with R_f values of 0.69 and 0.85 (solvent systems I, 100% light petroleum and II, light petroleum: DCM 90 : 10), respectively. The crystallization of these fractions using DCM-methanol mixture (1 : 1) afforded 500 mg of white waxy substance (compound **1**). Additionally, the fraction numbers 17–23 were eluted with 10% CH_2Cl_2/*n*-hexane using light petroleum: DCM 75 : 25 (III) and 100% DCM (VI) revealed the presence of one major spot with R_f values of 0.55 and 0.73, respectively. The pooled fractions were

purified by repeated crystallization from methanol as white crystalline scales (100 mg) compound **2**. Furthermore, fractions (31–37) eluted with 25% DCM/*n*-hexane revealed the presence of two major violet spots with R_f values (0.50 and 0.42, III) and (0.64 and 0.54, IV). These fractions were pooled, concentrated, and chromatographed on a silica gel column packed with 100% *n*-hexane and the polarity was gradually increased by DCM. Sub-column fractions (9–12) and (14–18) that were eluted with 25% DCM in *n*-hexane, revealed the isolation of two major spots, which were designated as compound **3** (white amorphous, 400 mg) and compound **4** (white granules, 100 mg), respectively. Moreover, column fractions 47–51 eluted with 40% DCM/*n*-hexane showed the presence of one major violet spot with R_f values (0.22, III and 0.40, IV). Repeated crystallization from methanol resulted in the purification of compound **5** as white scales with m.p. 63–64 °C. Also, the pooled fractions (61–65) eluted with 50% DCM/*n*-Hexane showed one major violet spot with R_f values 0.78 and 0.85 using solvent system V (DCM: methanol, 99 : 1) and VI (DCM: methanol, 98 : 2), respectively. The residue of pooled fractions was crystallized from DCM/methanol as colorless needles (200 mg, compound **6**) with m.p. 110–112 °C. Fractions (70–78) eluted with 100% DCM displayed one major spot with R_f values 0.65 (V) and 0.83 (VI). Purification was performed using repeated crystallization from the DCM/methanol mixture that yielded 500 mg of compounds **7** with R_f values 0.43 (V), 0.55 (VI), and m.p. 216–218 °C. Besides this, the fractions (90–95) eluted with 2.5% methanol/DCM revealed the presence of one major violet spot with R_f values 0.33 (V) & 0.45 (VI), A crystallized pooled fraction from methanol, afforded 500 mg of white needle-shaped crystals (compound **8**) with m.p. 136–138 °C. Finally, TLC examination of fractions 101–108 eluted by 10% methanol/DCM showed the presence of one major violet spot with R_f value 0.33 (VII, DCM: methanol 95 : 5) and 0.48 (VIII, DCM: methanol 85 : 15). The residue of the pooled fractions was crystallized from hot DCM/methanol afford 2 gm of white amorphous powder (compound **9**), as illustrated in Scheme S1.† All the isolated compounds were analyzed using EI/MS (Quadrupole mass analyzer in Thermo Scientific GC/MS model ISQ LT (USA) using Thermo Xcalibur software), ^{1}H-NMR and ^{13}C-NMR (Bruker (Switzerland)) at 400, 100 MHz, respectively. Chemical shifts are given in ppm with the TMS as an internal standard as well as, determination of m.p. (Digital, electro-thermal Ltd, England) for some isolated metabolites.

2.3. UPLC-ESI-MS-MS analysis of DCM-L and DCM-S fractions

The sample (100 µg mL^{-1}) solutions were prepared using high-performance liquid chromatography (HPLC) analytical-grade methanol solvent, filtered using a membrane disc filter (0.2 µm), then subjected to analysis based on the procedure that was previously reported.[11]

2.4. *In vivo* evaluation of the cardioprotective, anxiolytic, and anti-depressant activity of DCM-L and DCM-S fractions

2.4.1. Ethical approval. The study protocol was reviewed and approved by members of the Veterinary Institutional

Animal Care and Use Committee (VET-IACUC) of the Faculty of Veterinary medicine, Cairo University (approval number: Vet CU28/04/2021/272). Also, the procedures were in accordance with the National Institutes of Health guide for the care and use of Laboratory Animals (NIH Publications no. 8023, revised 1978).

2.4.2. Animals and experimental protocol. A total of 28 male rats were randomly distributed into four groups, seven animals in each, and all groups of animals were treated in the following manner: Group I – saline/normal control; rats were administered with normal saline (2 mL kg^{-1}, p.o. per day) for 21 days. Group II – ISO; rats were administered normal saline (2 mL kg^{-1}, p.o. per day) for 19 days. Group III – DCM-L and Group IV– DCM-S (200 mg kg^{-1}) +ISO; rats were treated with *M.* *macroura* DCM fraction of leaves and stem branches (200 mg kg^{-1}, p.o. per day) for 19 days. All groups except the group I were challenged with ISO (85 mg kg^{-1}, s.c.) on the 1st and 2nd day and treated with the corresponding treatment for 19 days. Twenty-four h after the last dose, all groups were subjected to behavioural assessment at 10 a.m. and continued for seven days. The dose and duration of ISO administration were selected according to previous studies.[10,12]

2.4.3. Determination of body weight and heart weight index (HWI). The body weight of rats in different groups was measured weekly and before euthanasia to determine their changes. After rat's dissection, the heart was gently excised, tapped between filter paper to remove any blood clots, weighed
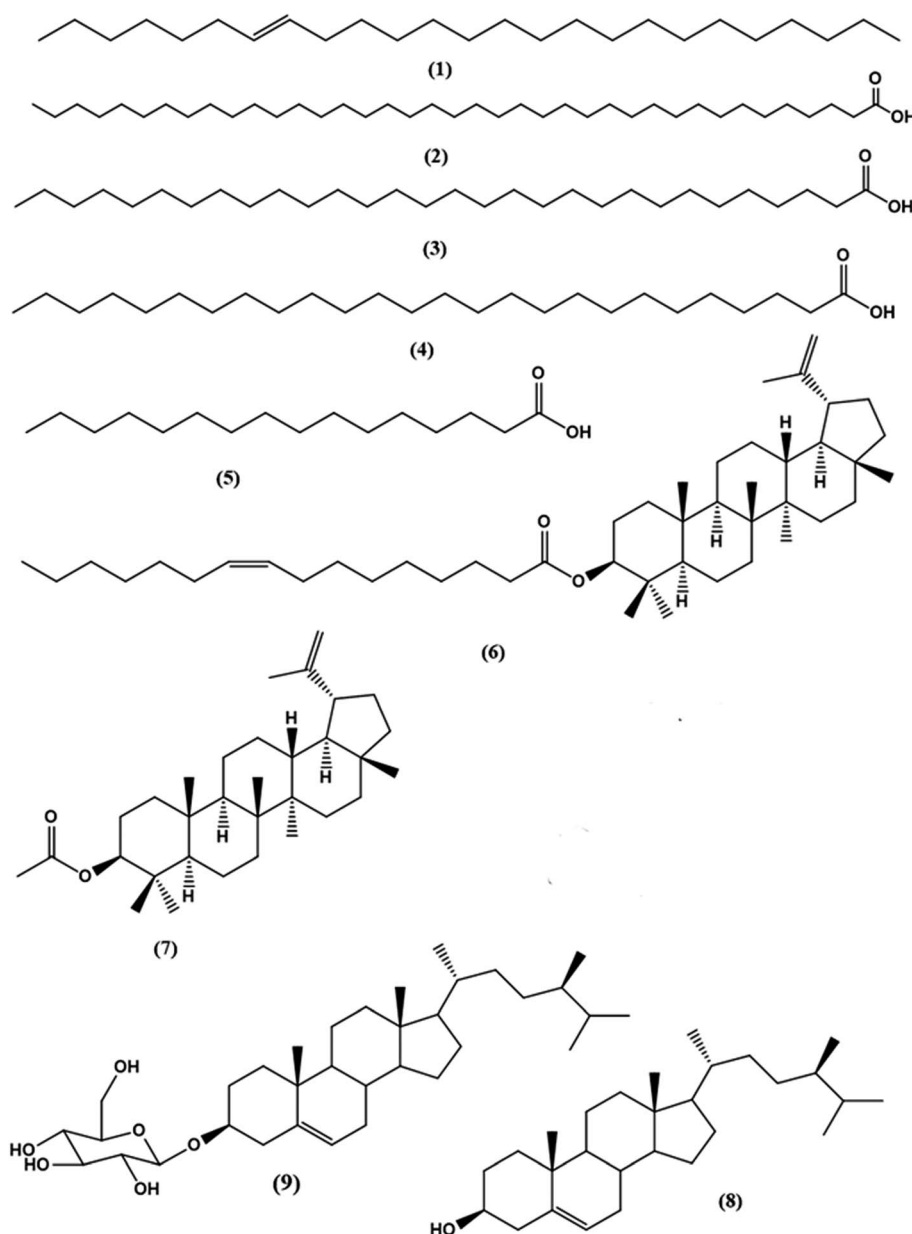

Fig. 1 Chemical structure of compounds isolated from DCM fraction of *Morus macroura*.

using a sensitive balance. Next, the HWI was calculated from the ratio of heart weight to the body weight of rats.

2.4.4. Behavioural testing. Rats were submitted to the behavioural research room and acclimatized to the environment before testing. All the tests were conducted by an experienced observer blind to the experimental treatments.

2.4.4.1. Anxiety like behaviour. Anxiety-like behaviour was determined using two behavioural tests. First, the open field test was used to measure the motor activity of rats. The measuring parameters were the number of crossings of the lines and frequency of rearing activity. The test duration was 3 min, and the procedures were conducted following the previous literature.[13] Then, the elevated plus-maze was tested. It

was dependent on the natural fear of rodents from heights. The recorded parameters were frequencies of entering the closed and open arms and durations for 5 min. The procedures and apparatus structure were following the previous ref. 11 and 14.

2.4.4.2. Depressive like behaviour. Depressive-like behaviour is performed using the forced swim test, which is a test of learned helplessness and used to screen the anti-depressant activity. Briefly, rats were tested in two sessions; the first is a training session for rats in a circular arena filled with warm water (27 °C) for 15 min. After 24 h, the second session (testing session) was performed where the mobility and immobility duration were recorded for 5 min.[15]
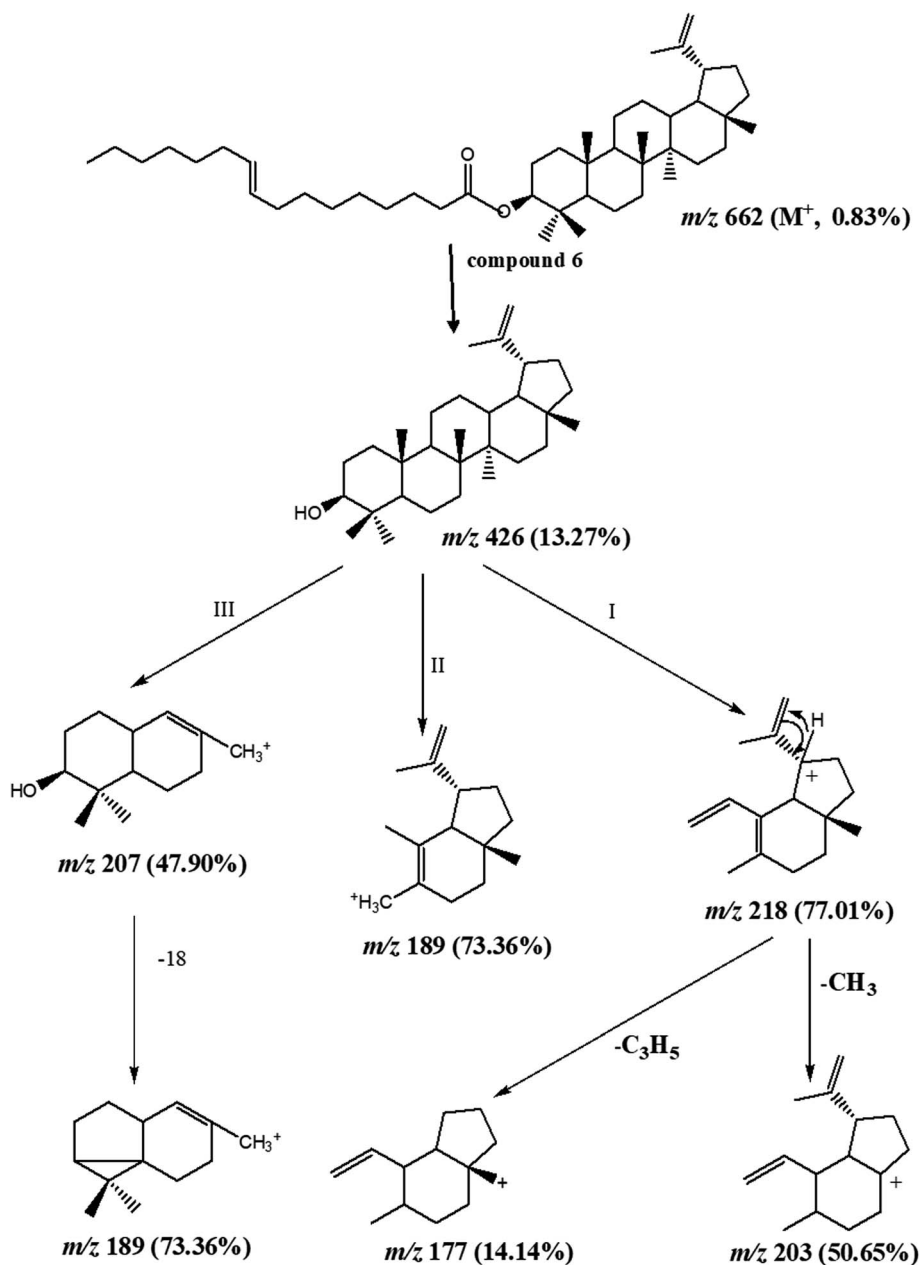

Fig. 2 Suggested mass fragmentation pattern of isolated compound **6**.

2.4.5. Animal sacrifice. After the last behavioural test, blood was collected from the inner canthus of the eye and centrifuged at 2504 × g and 4000 rpm for 10 min for serum separation to measure serum cardiac enzymes. Then rats were euthanized by cervical dislocation, and brains were excised gently, weighed, and homogenized in 75% aqueous HPLC grade methanol (10% w/v). Next, the homogenate was spun at 2504×g

and 4000 rpm for 10 min., and the supernatant was divided into two halves; the first was dried using a vacuum (70 Millipore) at room temperature and used for GABA (gamma-aminobutyric acid), while the second half was used for monoamine determination.

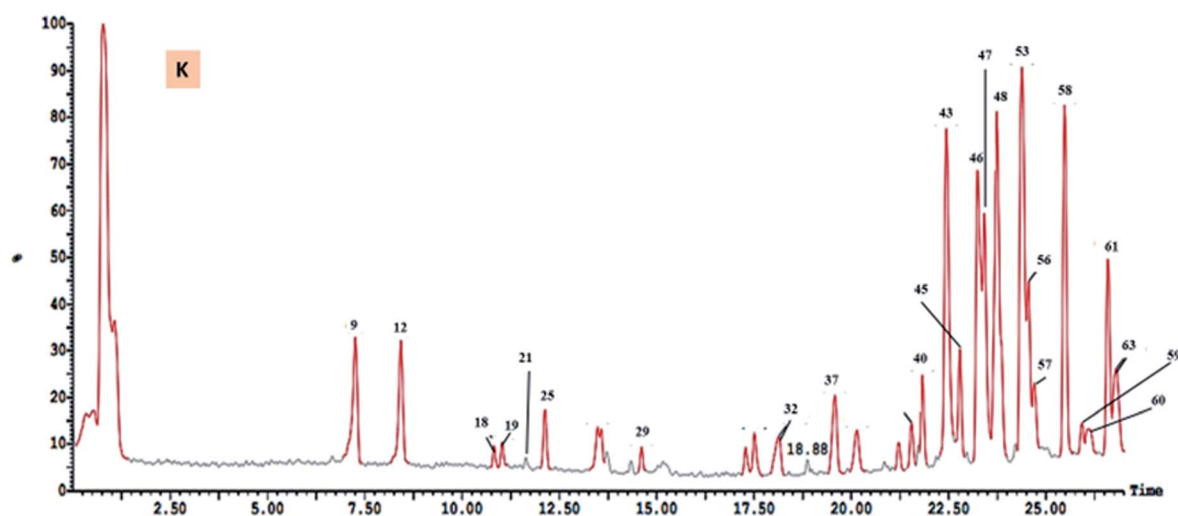**2.4.6. Biochemical evaluation.** Myocardial injury enzymes lactate dehydrogenase (LDH) and creatine kinase (CK) were
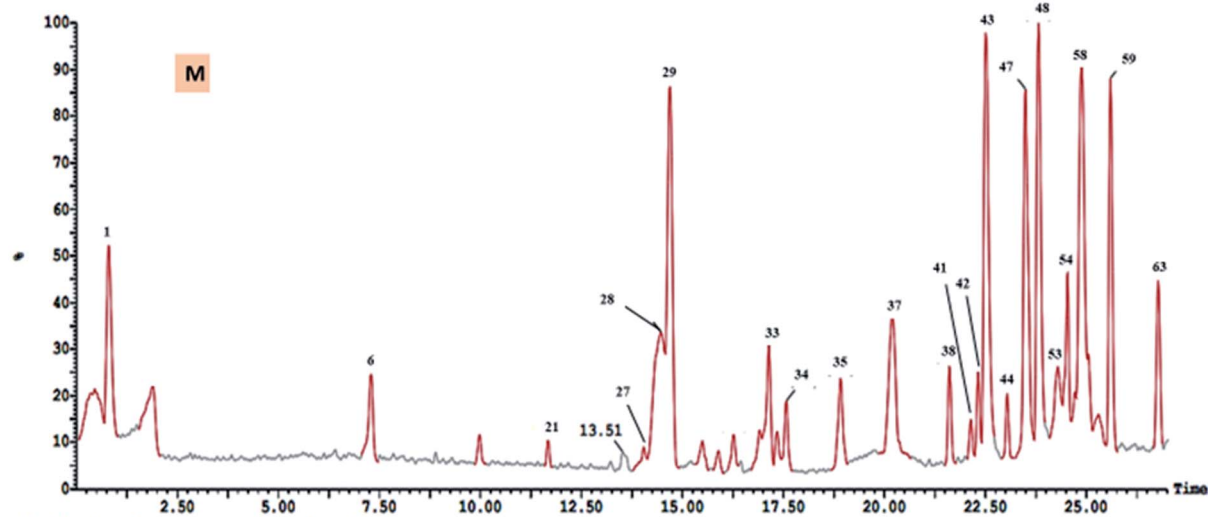

Fig. 3 UPLC-ESI-MS chromatograms of DCM fractions of leaves (K), and stem branches (M) of *M. macroura* Miq in positive ionization mode.

measured in the serum of rats. Also, brain oxidative stress, including superoxide dismutase (SOD) and reduced glutathione (GSH) as well as neuronal cell energy, were evaluated using HPLC.[16] Furthermore, the brain levels of GABA, serotonin, and dopamine were determined using HPLC.[17] Moreover, parts of the brain tissue were preserved in neutral buffer formalin (10%) for 48 hours before routine histological processing.

2.4.7. Histological examination. The formalized samples were dehydrated in ascending grades of ethyl alcohol, cleared in xylene, and embedded in paraffin wax. Sections of 3–4 μm in thickness were obtained by rotatory microtome, deparaffinized, stained with hematoxylin and eosin (H&E) stains for examination under a light microscope.[18]
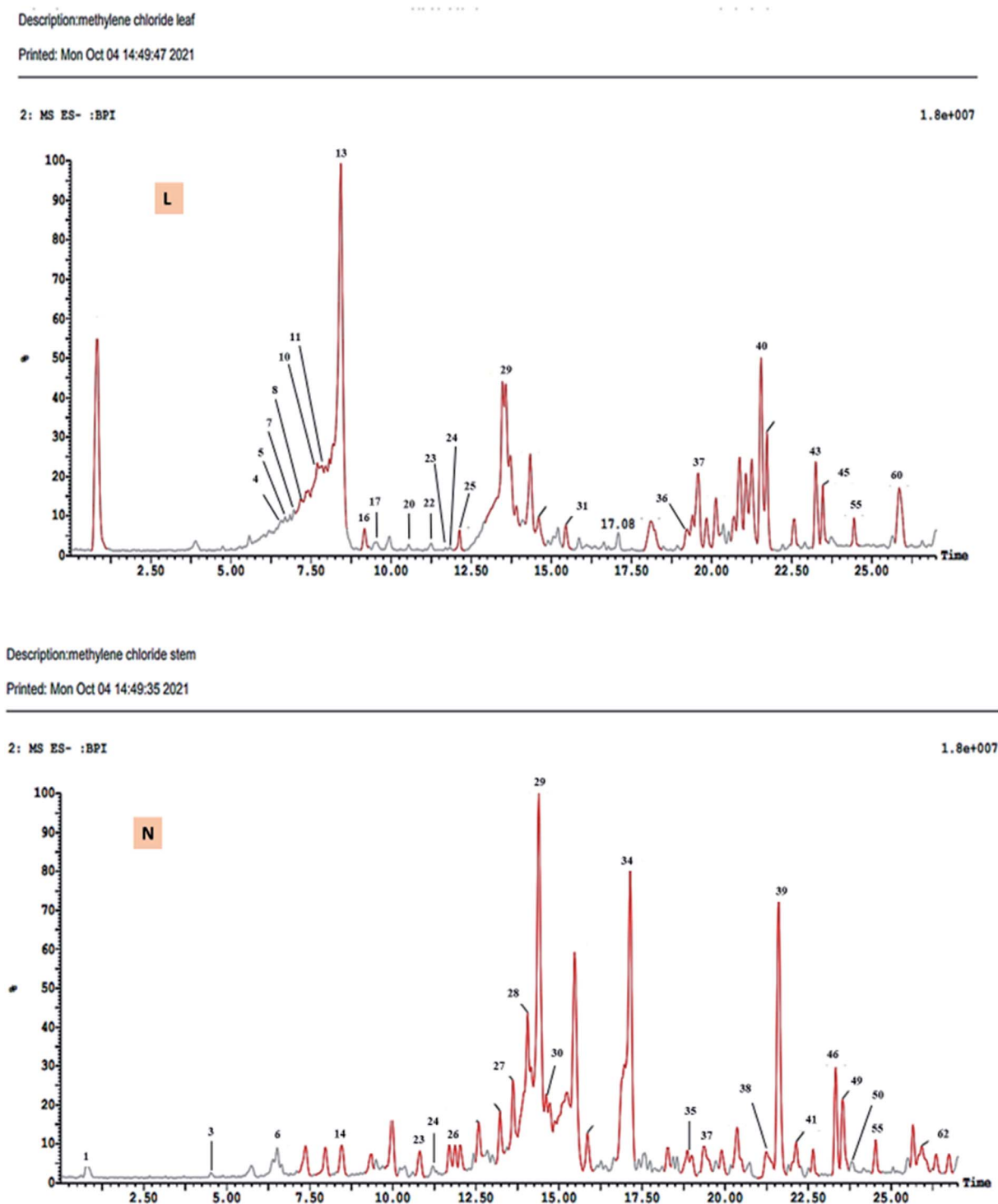

Fig. 4 UPLC-ESI-MS chromatograms of DCM fractions of leaves (L), stem branches (N) of *M. macroura* Miq in negative ionization mode.

Table 1 Compounds identified in the dichloromethane of leaves (DCM-L), and stem branches (DCM-S) of M. macroura by using UHPLC-ESI/MS/MS[a]

Peak no.	RT	RRT	MS$_1{}^{-/+}$	MS$_2$	Leaves	Stem branches	Tentative assignment
1	2.10	0.084	153/−	109	—	√	Protocatecheic acid
2	2.43	0.097	339/−	177 (100%)	0.95	—	*Aesculin
3	4.84	0.194	137/−	93 (100%)	—	0.51	Hydroxybenzoic acid
4	6.27	0.251	339/−	177 175 161,135 109	√	—	Morachalcone A
5	6.27	0.251	431/−	269 (100%)	0.95	—	*Apigenin-7-O-β-glucoside
6	6.73	0.269	163/165	119 (100%)	—	0.24	Coumaric acid
7	6.92	0.277	463/−	270.7	1.85	—	*Naringenin derivatives
8	7.26	0.291	447/−	285,256.9, 242.5,198.8	0.47	—	*Luteolin-7-O- glucoside
9	7.46	0.299	−/355	193	0.05	—	Scopolin
10	7.62	0.305	431/−	341, 311, 269	1.09	—	Apigenin-8-C-glucoside
11	7.92	0.317	463/−	301, 257	4.09	—	*Morin-O-β-glucoside
12	8.10	0.325	−/449	287	√	—	Cyanidin-3-O-glucoside
13	8.25	0.331	463/−	301 (100%)	7.33	—	Quercetin-3-O-β-D-glucoside
14	8.38	0.336	463/−	301	—	√	Quercetin-3-O-β-galactoside
15	8.96	0.359	431/−	269	0.01	—	*Apigenin-7-O- glucoside isomer
16	9.24	0.370	447/−	285	7.33	—	Kaempferol-3-O-β-glucoside
17	9.24	0.370	447/−	343, 301	0.47	—	Quercetin-8-C-rhamnoside
18	10.95	0.439	−/611	303, 328	0.80	—	*Hesperidin
19	10.95	0.439	−/610	317.5, 256.8, 151.2	√	—	*Petunidin dirhamnoside
20	11.14	0.446	447/−	301 255	0.41	—	Quercetin-3-O-β- rhamnoside
21	11.18	0.448	−/397	351	1.61	8.45	**Cerotic acid**
22	11.34	0.454	301/−	139 (100%), 256	0.41	—	Ellagic acid
23	11.34	0.454	355/−	193.3 (100%)	—	√	*Ferulic acid-O-glucoside
24	11.37	0.456	431/−	285 284, 255 227	—	√	*Kaempferol-3-O-β- rhamnoside
25	12.10	0.485	301/303	179, 151, 121	0.41	—	Quercetin
26	12.17	0.488	301/−	256,151 107	—	√	Morin
27	14.06	0.563	467/469	305	—	5.18	*Gallocatechin glycoside
28	14.15	0.567	467/469	305	—	5.18	*Epigallocatechin glycoside
29	14.39	0.577	329/−	287 [M–H–COCH$_3$]	2.30	13.36	Phloracetophenone-4-O-glucoside
30	14.68	0.588	575/−	—	—	1.05	β-Sitosterol-3-O-β-D-glucoside
31	16.04	0.643	467/−	—	0.27	—	Lupeol acetate
32	17.77	0.712	−/579	—	1.78	—	**Nonatriacontanoic acid**
33	17.83	0.715	353/355	203	—	√	*Epoxybergamottin
34	17.83	0.715	353/355	299, 69	—	0.62	Albanin A
35	18.38	0.737	293/295	220.8 (100%)	—	0.01	*Hydroxy octadecatrienoic acid
36	18.87	0.756	591/−	287	√	—	*Cyanidin cinnamoyl glucuronide
37	19.77	0.792	317/−	—	0.86	1.73	Unknown
38	21.08	0.845	475/477	299.0	—	0.67	*Chrysoeriol-uronic acid
39	21.40	0.858	433/−	271	—	√	*Naringenin-7-O-β-glucoside
40	21.49	0.861	379/381	318, 163, 71, 69	1.61	—	*Brassicasterol
41	21.99	0.881	475/477	255	—	0.67	Palmitic acid ester
42	22.73	0.911	−/683	331	—	√	*Malvidin diglucoronide
43	23.02	0.922	451/-	249.8 390.5 406.7 435.1	0.80	16.23	**Melissic acid**
44	23.06	0.924	-/683	597, 435, 287	—	0.88	*Cyanidin derivative
45	23.24	0.931	255/−	—	2.10	2.81	Palmitic acid
46	23.47	0.941	281/−	—	1.08	2.14	Oleic acid
47	23.55	0.944	−/391	279, 149 (100%)	4.49	8.30	*Bis (2-ethyl hexyl) phthalate
48	23.72	0.951	−/593	287 434, 595	9.12	8.45	Cyanidin rutinoside
49	23.83	0.955	349/−	—	1.08	2.14	**Pentacos-7-ene**
50	23.86	0.956	395/−	281	—	√	Oleic acid ester
51	24.14	0.967	−/607	286	0.23	2.48	Australisine A
52	24.44	0.979	283/−	239 [M–H–COO]	0.52	0.82	Octadecanoic acid
53	24.65	0.988	−/535	317, 153	6.30	6.32	*Isorhamnetin-3-O-acetyl glucuronide
54	24.65	0.988	−/536	317, 153	—	0.02	*Petunidin 3-O-acetyl glucuronide
55	24.95	1.000	339/−	163 (100%)	4.75	8.66	Euchrenone a7
56	25.29	1.013	−/397	254.9	3.90	2.99	**β-Sitosterol**
57	25.47	1.020	−/535	331	6.30	6.32	*Malvidin-3-O-acetylglucuronoide
58	25.53	1.023	−/683	597(loss of 86), 435 (loss of glucose), 287.7	10.15	12.42	*Cyanidin-3-O-malonyl glucoside derivative
59	25.84	1.035	−/535	287	6.99	15.18	*Cyanidin-3-O-malonyl glucoside
60	26.34	1.055	661/663	—	0.30	—	**Lupeol palmitate**
61	26.59	1.065	−/611	287, 449	3.90	2.99	*Cyanidin-3-O-hexosyl hexoside
62	26.82	1.075	475/−	299.8, 429	—	0.67	*Peonidin-3-O-glucuronide

Table 1 (Contd.)

Peak no.	RT	RRT	$MS_1^{-/+}$	MS_2	Leaves	Stem branches	Tentative assignment
63	27.68	1.109	−/398	314	6.40	9.35	*24-Methylene-ergosta-5-en-3β-Ol
64	28.13	1.127	455/−	400.5	—	8.66	Oleanolic acid

[a] *Compounds identified for the first time in the family Moraceae. Bold with or without * means compounds isolated as pure metabolites from *M. macroura*. √ Minor compounds. — Compounds not detected.

A scoring system to evaluate the myocardial injuries in rats caused by ISO was assessed.[19] The findings were classified into the following degrees to compose a range of histologic myocardial injury considering (0 : 3) scores for the categories; edema, myocardial necrosis, and inflammatory cell infiltrates. The score (0 : 3) was assigned to (0) no damage, (1) slight damage, (2) moderate damage, and (3) maximum damage. This method was used for estimating the HP index in the heart.

2.5. Statistical analysis

All quantitative results were analyzed using the SPSS version 17.0 for Windows. Data were presented as mean ± SEM. Comparisons among multiple group means were performed using a one-way analysis of variance, followed by the Bonferroni test as a post hoc test. Statistical significance was set at $p \leq 0.05$.

3. Results and discussion

Our study aimed to investigate the possible cardioprotective and anti-depressant effects of DCM-L and DCM-S fractions of *M. macroura*. in an ISO induced post-MI depression-rat model. This study was reinforced by the chromatographic technique of these fractions, which afforded the isolation and identification of nine secondary metabolites belonging to fatty acids and their derivatives, steroid, and triterpenoid compounds. In addition, the UPLC-ESI-MS-MS profile of DCM-L and DCM-S fractions that were analyzed separately afforded the identification of 42 and 41 secondary metabolites, respectively. The flavonoids and anthocyanins are the major metabolites identified in *M. macroura*.

3.1. Phytochemical study

Column chromatography of the combined DCM fractions resulted in the isolation of nine compounds, namely; lupeol palmitate (**6**). It is isolated for the first time from nature with eight known compounds including pentacos-7-ene (**1**), non-atriacontanoic acid (**2**), melissic acid (**3**), cerotic acid (**4**), palmitic acid (**5**), lupeol acetate (**7**), β-sitosterol (**8**), β-sitosterol-3-*O*-β-D-glucopyranoside (**9**) (Fig. 1 and Schemes S1† and S texts 1–10). Where, fractions eluted with 50% CH_2Cl_2/*n*-hexane afforded 200 mg of colorless needles of compound **6** with m.p. 110–111 °C and R_f 0.78 & 0.85 using solvent system (DCM: methanol 99 : 1) and (DCM: methanol 98 : 2). Moreover, the physical and chemical characteristics of compound (**6**) suggested a steroidal or triterpenoidal skeleton. The EI-MS spectrum showed M^+ at *m/z* 662 corresponding to molecular formula $C_{46}H_{78}O_2$ and characteristic fragments at *m/z* 426 for [M^+-236], where 218, 207, 203,

189, and 177 that are characteristic for triterpenoidal skeleton as illustrated in Fig. 2.[20] ^{1}H-and ^{13}C-NMR spectral data showed signals at δ_H 4.26, δ_C 79.17 for H-3 and C-3, respectively, and an exocyclic double bond at δ_H 4.69, 4.57 with corresponding olefinic carbons at δ_C 131.03 and 132.61 with other ^{1}H-NMR signals confirmed the presence of lupeol as the triterpenoidal compound.[21] The downfield shift of the proton at C-3 (δ_H 4.26 ppm) and the carbonyl group at δ_C 167.91 indicated the presence of an esterified hydroxyl group at this position. The ^{13}C-NMR spectral data showed characteristic thirty carbons for lupeol nucleus with M^+ 426 in addition to other sixteen signals for the acidic moiety [with *m/z* 236 ($C_{16}H_{30}O$)]. The double bond position is deduced from the loss of 26 amu between *m/z* 85 (C_6H_{13}) and *m/z* 111 (C_8H_{15}). This proved that the double bond is between C-9′ and C-10′. The consequent losses of 14 or 28 amu and the presence of the C=O group confirmed that we dealt with palmitoleic acid moiety.[22] From the previous spectral data, compound (**6**) could be identified as lupeol palmitoleate ($C_{46}H_{78}O_2$).

3.2. Characterization of metabolites from DCM-L and DCM-S analyzed by UPLC-ESI-MS-MS

The DCM fractions obtained from leaves and stem branches of *M. macroura* were profiled by UPLC- ESI-MS/MS using negative and positive ionization modes (Fig. 3 and 4). Altogether, 64 metabolites were identified depending on the MS–MS fragmentation pattern and data published in the literature. The compounds are summarized and ordered in Table 1 according to their relative retention time (RRT), calculated according to Euchrenone a7. The characterization of secondary metabolites identified in the DCM fraction of leaves and stem branches is explained in detail in ESI; S texts 11–23.†

3.3. Biological study

3.3.1. Body weight, HWI, myocardial enzymes, and histopathological profile of MI rat model. ISO exposed rats displayed a marked reduction in their body weights compared to control rats. However, DCM-L200 treated rats showed a steady increase in their body weights compared to DCM-S200 treated rats (Fig. 5a). Concerning HWI, ISO and DCM-S200 exposed rats showed a substantial increase in their HWI compared to control rats. On the other hand, no significant difference was found between DCM-L200 treated rats and control rats (Fig. 5b). This result is attributed to the extensive edema caused by ISO in the myocardium followed by inflammatory cell invasion, which leads to myocardial hypertrophy.[23–25]

However, the administration of DCM-L200 was able to reduce the edematous inflammation and, therefore decreased the HWI.

Concerning myocardial enzymes, ISO exposed rats displayed an increase in LDH and CK-MB levels compared to the control group. The increased serum myocardial enzyme levels upon ISO
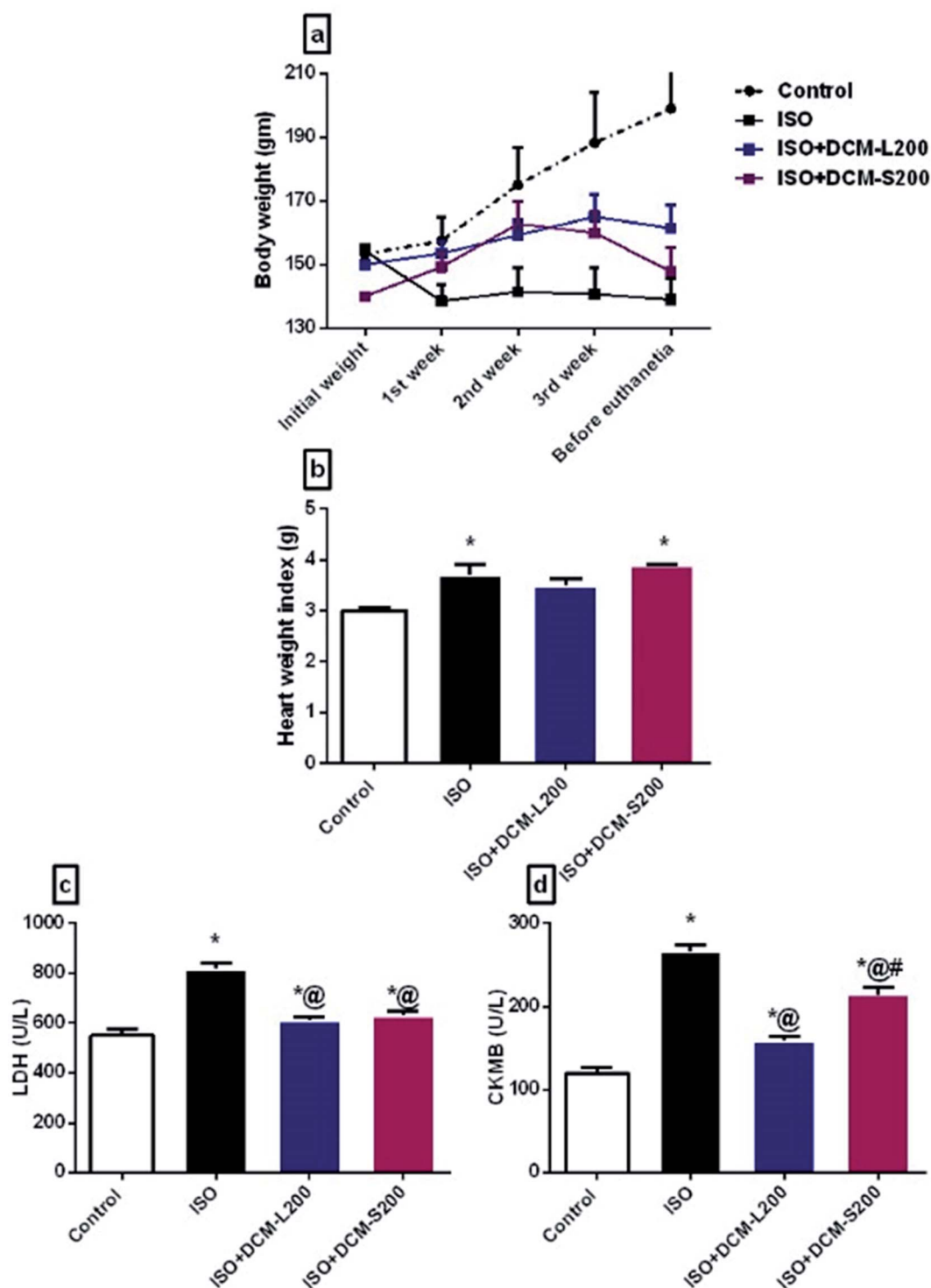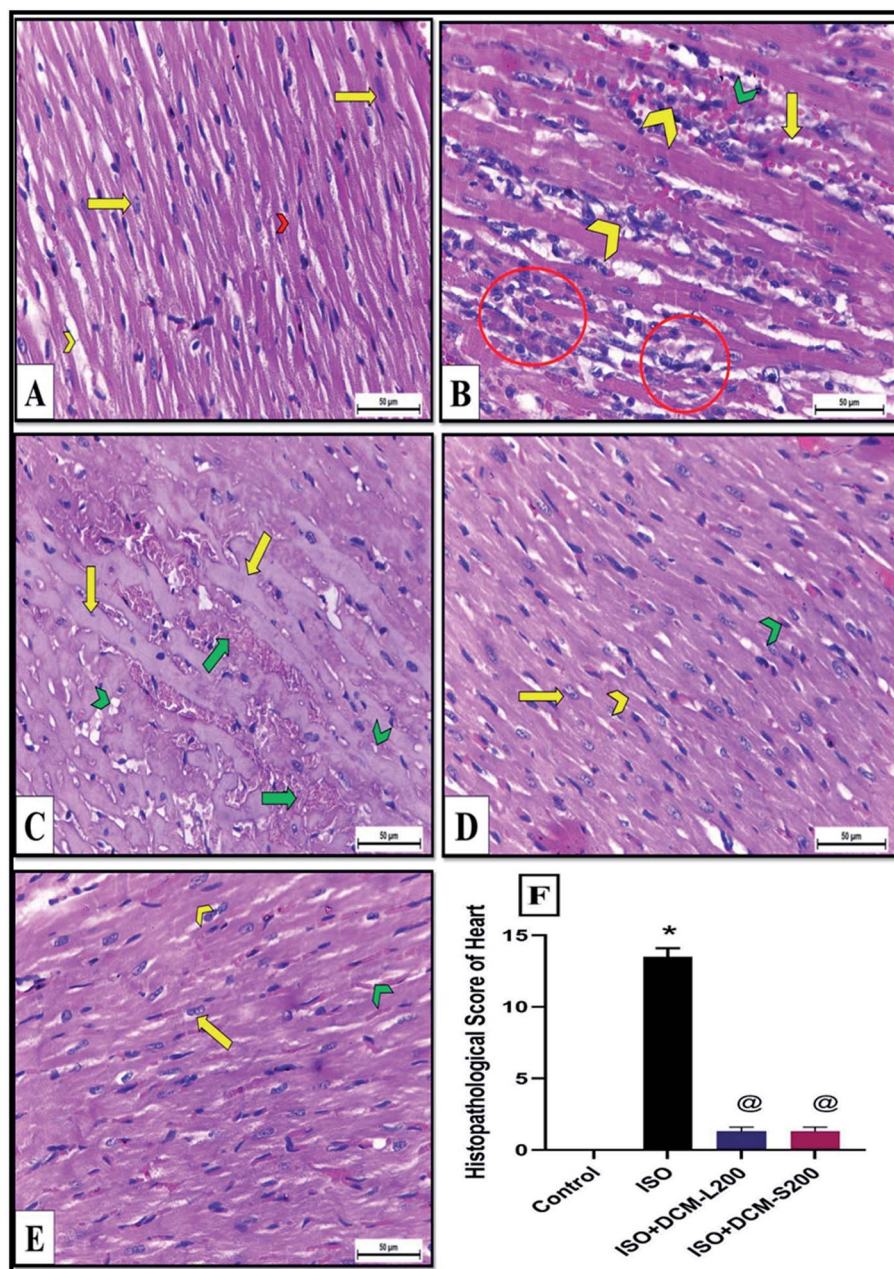

Fig. 5 Effect of DCM-L and DCM-S fractions of *M. macroura* on the body weight, heart weight index and myocardial enzymes of ISO induced post MI depressed rat. (a) Body weight, (b) heart weight index, (c) lactate dehydrogenase, and (d) creatine kinase. Data are expressed as mean ± SEM, one-way ANOVA followed by post hoc test Bonferroni test for seven rats in each group. * Significant from control group, and @ Significant from Iso group. $p < 0.05$.

administration at a dose of 85 mg kg^{-1} reflect the degree of myocardial injury.[26] The elevated myocardial enzyme levels could be attributed to the ability of ISO to produce free radicals *via* the adrenoceptor mechanism. Also, ISO affects the cell metabolism to such a degree that cytotoxic free radicals are formed, producing myocardial necrosis.[27] On the other hand, the administration of DCM-L and DCM-S fractions at a dose of

200 mg kg^{-1} were able to reduce the CKMB and LDH levels with superiority to DCM-L in reducing CKMB levels compared to DCM-S (Fig. 5c and d).

These enzymes leakage in the ISO exposed rats were associated with severe degenerative changes in cardiac myocytes, including lymphocytic infiltration, hemorrhage, wavy-shaped myofibers with unclear striation, some myofibers that

Fig. 6   (A–F) Cardiac muscles of albino rats H&E X400. A: Control rats showing normal elongated branched and cross striated myofibers with oval central nuclei (yellow arrow) and narrow slit-like interstices (yellow chevron) in between (B and C) ISO exposed rats revealing degenerative changes included (B) lymphocytic infiltrations (yellow chevron), hemorrhage (green chevron), wavy-shaped myofibers with unclear striation (yellow arrow), and some myofibers that appeared necrotic (circle). (C) Amyloidosis of cardiac myofibers (yellow arrow) with severe hemorrhage (green arrow). There was cytoplasmic vacuolation in cardiac myocytes (green chevron). (D) ISO + DCM-L200 and (E) ISO + DCM-S200 treated rats showing significant recovery evidenced by nearly normal-shaped striated cardiac myofibers (yellow chevron) with elongated nucleus (yellow arrow) and interstices between myofibers contained few hemorrhages (green chevron). (F) Histopathological score between the four groups, data are expressed as mean ± SEM. * Significant from control group, and @ Significant from ISO group. $p < 0.05$.

appeared necrotic, and cytoplasmic vacuolation as shown in Fig. 6B and C. These findings are in agreement with the previously published works.[28–30] Conversely, cardiac muscle sections of DCM-L200 and DCM-S200-treated rats showed significant recovery evidenced by nearly normal-shaped cardiac myofibers that appeared elongated, branched, striated, and contained oval

central nuclei. However, few hemorrhages were observed at the interstices between myofibers (Fig. 6D and E). The cardiac muscle histopathological score was significantly higher in ISO exposed rats than in control rats. However, the score was significantly lower in rats treated with DCM-L200 and DCM-S200 compared to ISO exposed rats (Fig. 6F).
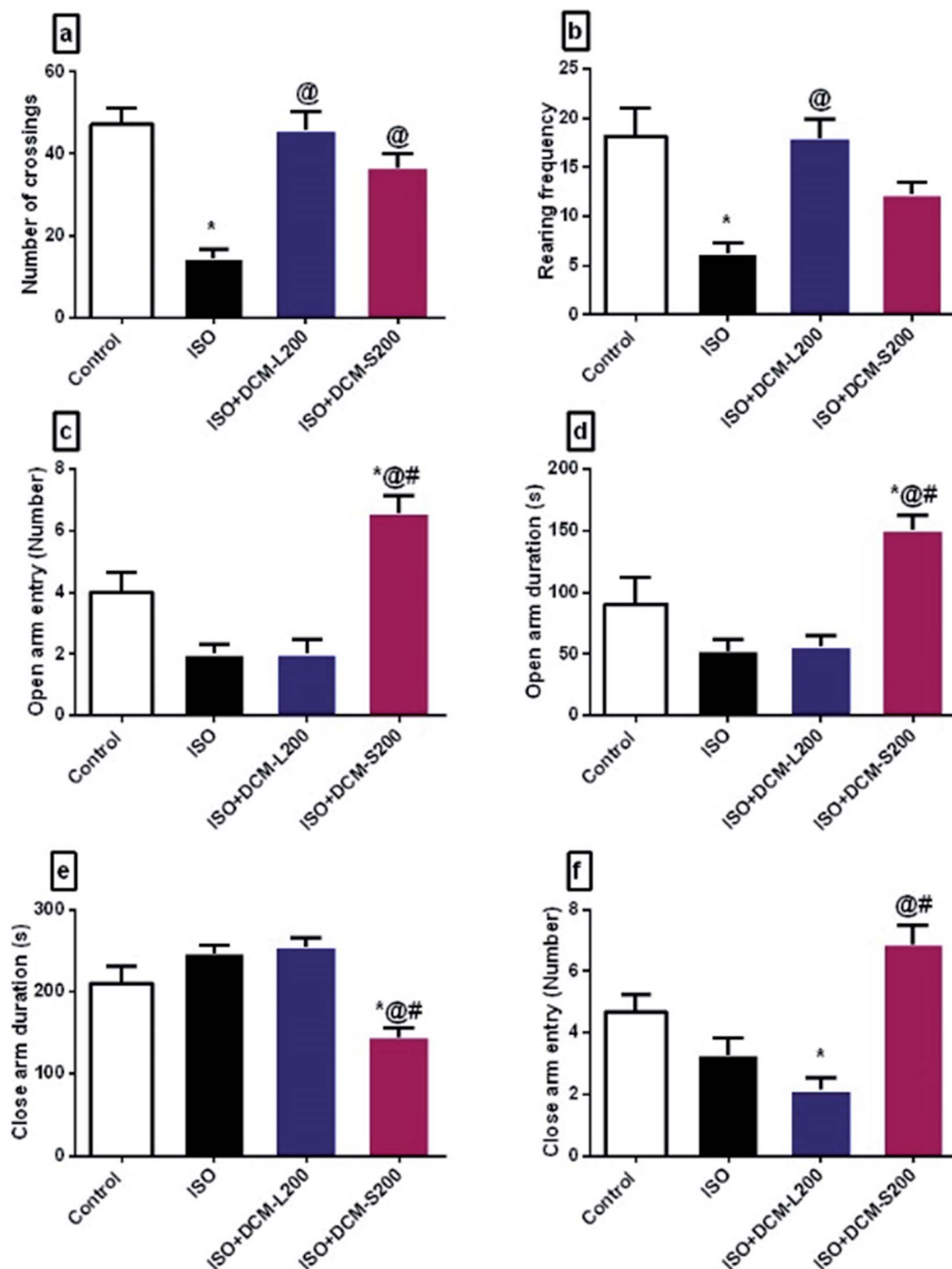

Fig. 7 Effect of DCM-L and DCM-S fractions of *M. macroura* on the motor activity and anxiety like-behaviour of ISO induced post-MI depressed rat. (a) Number of crossings, (b) rearing frequency, (c) open arm entry, (d) open arm duration, (e) close arm entry, and (f) Close arm duration. Data are expressed as mean ± SEM, one-way ANOVA followed by post hoc test Bonferroni test for seven rats in each group. * Significant from control group, @ Significant from ISO group, and # significant from ISO + DCM-L200, $p < 0.05$.
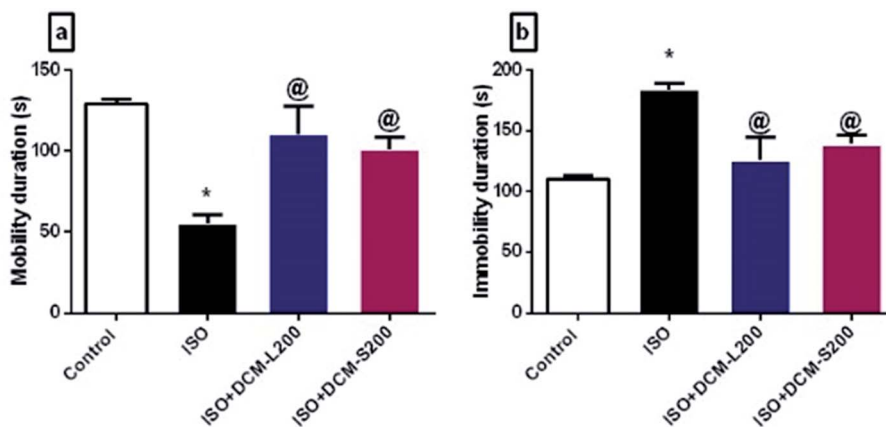
Fig. 8 Effect of DCM-L and DCM-S fractions of *M. macroura* on the depressive like behaviour of ISO induced post MI depressed rat. (a) Mobility duration, and (b) immobility duration. Data are expressed as mean ± SEM, one-way ANOVA followed by post hoc test Bonferroni test for seven rats in each group. * Significant from control group, and @ Significant from ISO group. $p < 0.05$.
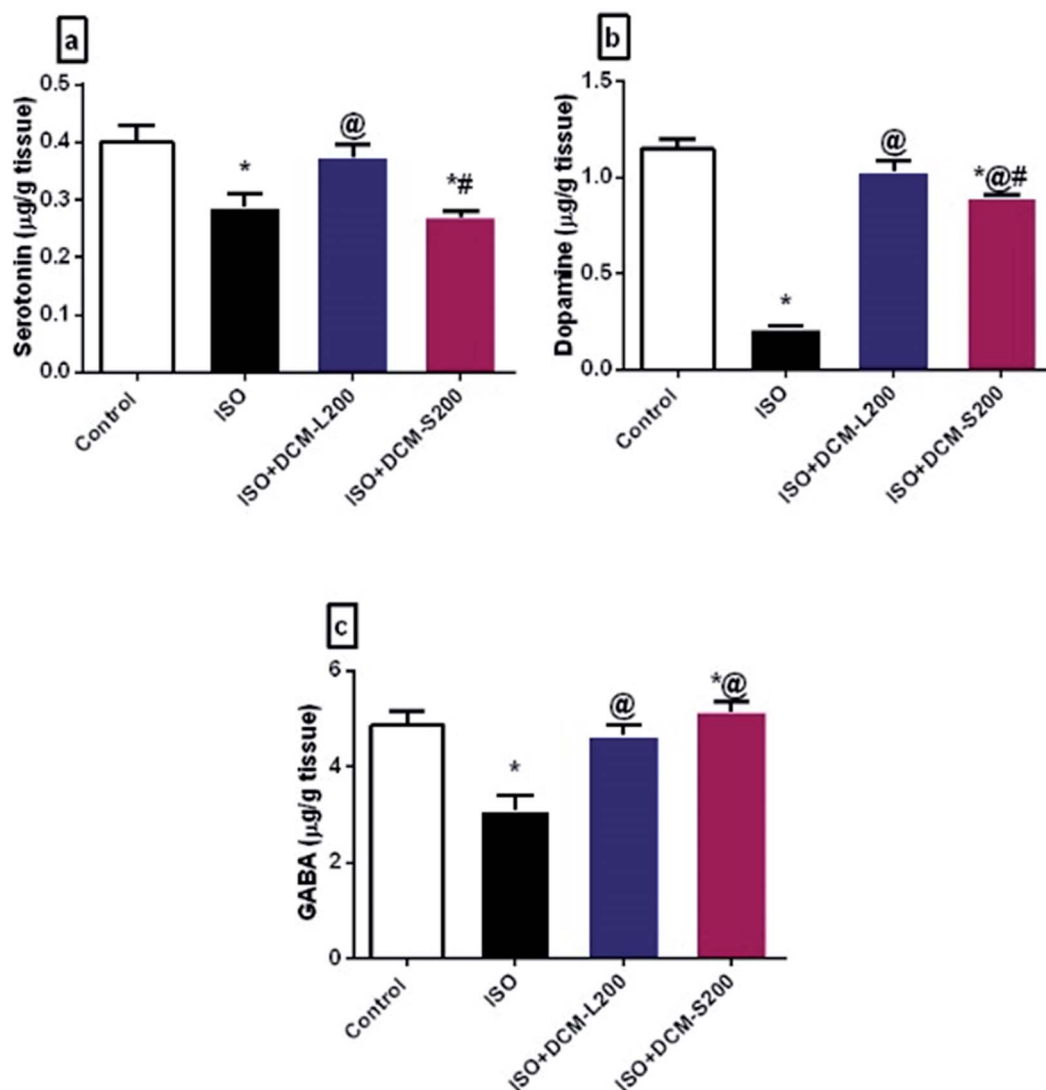

Fig. 9 Effect of DCM-L and DCM-S fractions of *M. macroura* on brain catecholamine, monoamine and inhibitory amino acid of ISO induced post MI depressed rat. (a) serotonin, (b) dopamine, and (c) GABA. Data are expressed as mean ± SEM, one-way ANOVA followed by post hoc test Bonferroni test for seven rats in each group. * Significant from control group, @ Significant from ISO group, and # significant from ISO + DCM-L200, $p < 0.05$.

Fig. 10 Effect of DCM-L and DCM-S fractions of *M. macroura* on the altered neuronal cell energy and brain oxidative stress of ISO induced post MI depressed rat. (a) Adenosine triphosphate (ATP), (b) superoxide dismutase, and (c) reduced glutathione. Data are expressed as mean ± SEM, one-way ANOVA followed by post hoc test Bonferroni test for seven rats in each group. * Significant from control group, @ Significant from ISO group, and # significant from ISO + DCM-L200, $p < 0.05$.
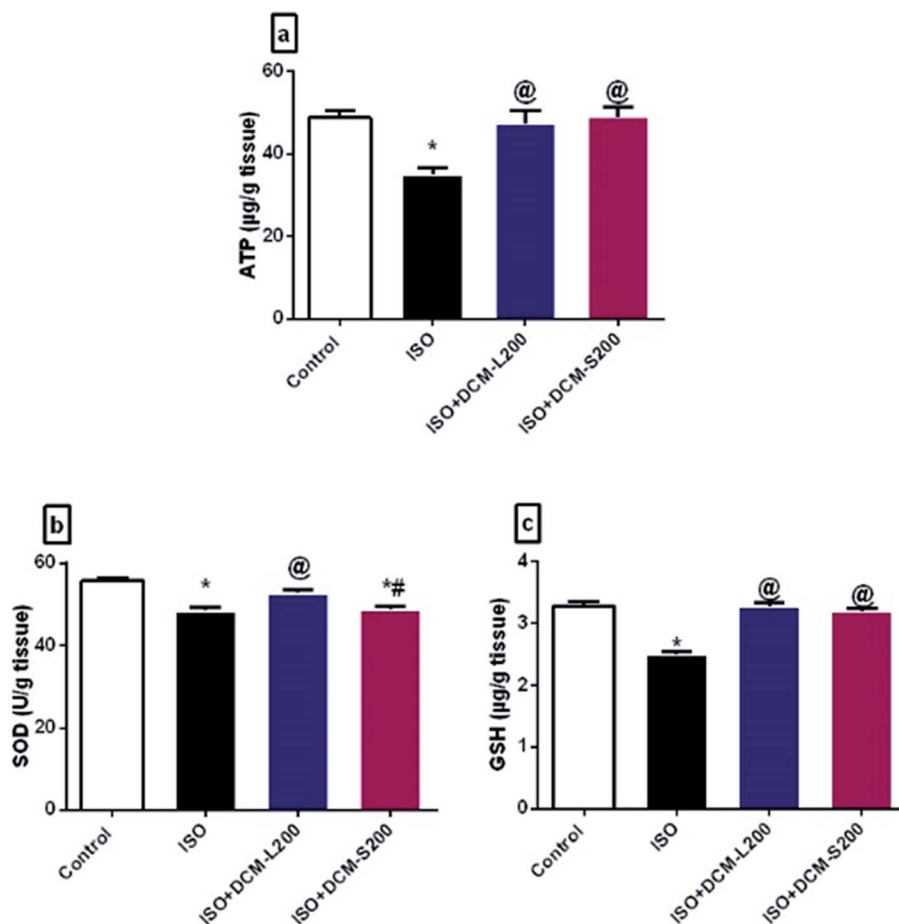
3.3.2.   Behavioural, neurochemical, and histopathological features of the post-MI depression rat model. There is a direct association between anxiety and depressive disorders and patients with cardiovascular diseases, including MI.[31] In rodents, anxiety-like behaviour can be measured using an open field test and elevated plus-maze.[32] The two tests depend on the natural fear of rodents from exposed areas and the height places. Likewise, depressive-like behaviour can be measured using a forced swim test, a test of learned helplessness, and can be used as a screening tool to detect the anti-depressant activity of novel agents.[33] Herein, ISO exposed rats displayed a reduction in the general motor activities, including the number of crossing squares and rearing frequency in the open field test and decreased frequency of open arm entries and duration spent in the elevated plus-maze open arms (Fig. 7a and b). These behavioural changes reflect the general anxious state of the ISO exposed rats. These data were in agreement with previous studies,[34,35] who induced MI surgically by coronary artery ligation and assessed anxiety-like behaviour using open field test and elevated plus-maze. However, the administration of DCM-L and DCM-S fractions were able to restore the
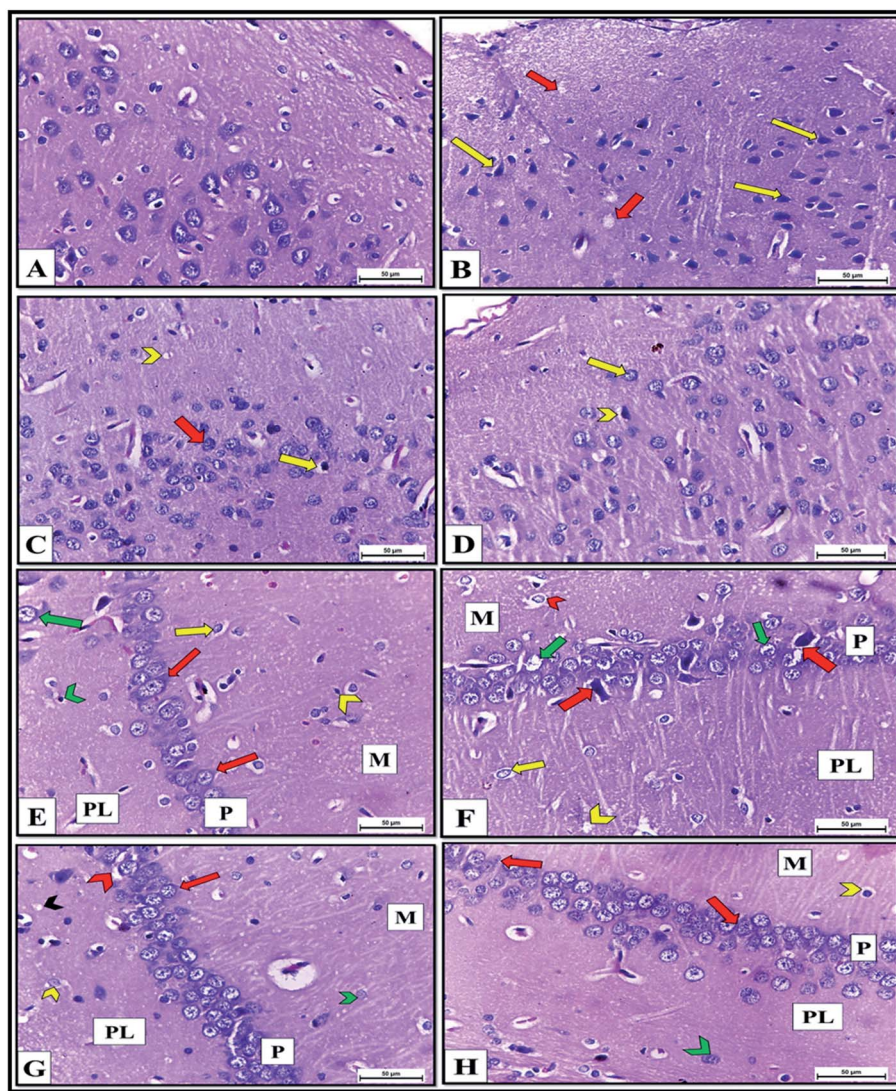
emotional stability of the rats as visualized by increasing the general locomotor activities in the open field test. Surprisingly, the activity of DCM-L treated rats was comparable to ISO exposed rats' activity in the elevated plus-maze in terms of frequency of entering closed arms and open arms and durations in both arms (Fig. 7c–f). However, the activity of DCM-S treated rats was superior to the activity of DCM-L treated rats. These findings support the anxiolytic activity of the DCM-S fraction *versus* the DCM-L fraction.

Concerning the behaviour of rats in the forced swim test, ISO exposed rats displayed a depressant-like behaviour in terms of decreasing the mobility duration and increasing the immobility duration. This was consistent with the previously published literature.[35] However, administration of DCM-L and DCM-S fractions increased the mobility duration and reduced the immobility duration with superiority to DCM-L *versus* DCM-S, although the difference between both fractions is not significant (Fig. 8a and b).

There are several possible explanations for these behavioural findings. First of all, the disturbance in the neurotransmitter system was associated with anxiety and depression.[36] The

Fig. 11 (A–D) Cerebral cortex sections of albino rats H&E X400. (A)Control rats showing normal structure and distribution of cerebral cortex neurons and neuropil. B: ISO exposed rats revealing neuropil vacuolation (red arrow) and pyknosis of pyramidal cells with pericellular space (yellow arrow). (C)DCM-L200 treated rats showing marked recovery evidenced by diminish of neuropil vacuolation (chevron), pyramidal cells restored its normal shape with vesicular nuclei (red arrow) and few neurons still pyknotic with pericellular space. D: DCM-S200 treated rats revealing marked recovery represented by nearly normal neurons with vesicular nuclei (yellow arrow) but few neurons still pyknotic with pericellular space (chevron) (E–H) Hippocampus sections of albino rats H&E X400. (E)Control rats showing normal structure of; molecular layer (M) that contained neurons (yellow arrow) and glia cell (chevron), pyramidal layer (P) that consisted of triangular shaped cells with central spherical nuclei had prominent nucleoli (red arrow) and polymorphic cell layer (PL) that consisted of neurons (green arrow) and glia cells (chevron). (F)ISO exposed rats revealing chromatolysis of neurons that were surrounded by pericellular spaces (chevron) in molecular (M) and (yellow arrow) in polymorphic layers (PL). The pyramidal cell layer (P) contained shrunken and pyknotic neurons (red arrow), and some pyramidal neurons had karyolitic nuclei (green arrow). Spongiform vacuolation of neuropil (chevron) was observed in polymorphic layer (PL). G: DCM-L200 treated rats showing great restore of the shape of the neurons in M layer (green chevron), in (P) layer (red arrow), and PL (yellow chevron) but few neurons appeared with pericellular space (red chevron). Negligible neuropil vacuolation (black chevron) was observed. H: DCM-S200 treated rats exhibiting marked restore of the shape of the neurons in (P) layer (red arrow) and PL (green chevron) with few neurons with pericellular space (yellow chevron).

decreased serotonin levels in the brain tissues are considered the major contributor to depression pathogenesis.[37] In addition, the dopamine system contributes to some depression symptoms, such as decreasing motivation. Both serotonin and dopamine are responsible for the emotional well-being of humans.[38] Herein, ISO exposed rats decreased the serotonin and dopamine brain levels due to endogenous homeostasis for

adapted the inotropic effects and Ca^{2+}-dependent mechanisms, as reported previously.[39] However, the administration of DCM-L and DCM-S fractions boosted the serotonin and dopamine brain levels (Fig. 9a and b).

Another possible explanation for the behavioural alterations of ISO exposed rats is the disruption of GABA neurotransmitters. GABA is an inhibitory neurotransmitter responsible for the

flow of information through the brain due to its extrinsic control.[40] This finding is consistent with many clinical and pre-clinical studies that report the direct relationship between the reduced brain GABA levels and depression.[40,41] However, administration of DCM-L and DCM-S fractions could increase the brain levels of GABA (Fig. 9c).

Moreover, a direct relationship exists between depletion of neuronal cell energy and depression.[42] Energy requirements for neurotransmitter release are controlled by the levels of ATP.[43] In our study, ISO exposed rats exhibited a decreased level of ATP. This finding agrees with previous literature and is confirmed by reducing serotonin and dopamine brain levels.[44,45] However, the administration of DCM-L and DCM-S increased ATP brain levels (Fig. 10a).

Oxidative stress is involved in many brain disorders, including depression, due to the high susceptibility of the brain to the reactive oxygen species (ROS).[46] In this study, ISO exposed rats displayed decreased SOD and GSH brain levels.[47] While the administration of DCM-L and DCM-S increased the SOD and GSH brain levels (Fig. 10b and c).

The histopathological picture of brain tissue, including the cerebral cortex and hippocampus, also confirmed the neurochemical disturbance in the brains of the ISO exposed rats. It revealed pyknosis and shrunken neurons with neuropil vacuolation (Fig. 11B). These structural abnormalities agree with previous findings,[48] reporting that decreased neurogenesis and neurite outgrowth in the ventral hippocampus are associated with heart failure in rats. Meanwhile, cerebral cortex sections of DCM-L200 and DCM-S200-treated rats showed marked recovery, evidenced by a significant decrease in the neuropil vacuolation, pyramidal cells restored their normal shape with vesicular nuclei. However, few cells appeared pyknotic with pericellular space (Fig. 11C and D). Also, histological examination of H&E-stained hippocampus sections of control rats showed three layers; molecular, pyramidal, and polymorphic layers, respectively (Fig. 11E).

In contrast, hippocampus sections obtained from ISO exposed rats revealed histopathological changes such as chromatolysis of neurons surrounded by pericellular spaces in molecular and polymorphic layers. The pyramidal cell layer contained shrunken, pyknotic neurons, and some pyramidal neurons had karyolitic nuclei. Also, spongiform vacuolation of neuropil was observed (Fig. 11F). However, hippocampal sections of DCM-L200 and DCM-S200-treated rats exhibited great restoration of the shape of the neurons in the three layers, but few neurons appeared with pericellular space. However, Neuropil vacuolation was reduced to a greater extent (Fig. 11G and H).

In conclusion, Genus *Morus* is an enriched phytochemical plant and plays a significant role as a diet-based therapy to cure various disorders. The presence of phenolic compounds, including flavonoids, quercetin, and its derivatives, is responsible for the *Morus* cardioprotective potential,[49] *via* several mechanisms: antioxidant, anti-apoptosis, anti-inflammatory, inhibition of mitochondrial dysfunction, and DNA damage.[50] Additionally, the presence of fatty acids, including melissic acid and cerotic acid, played a role in the cardioprotective and anti-

depressant actions of *Morus*.[51,52] Also, β-sitosterol, an isolated compound, was reported as a cardioprotective drug by reducing myocardial infarcted size, inflammatory mediators, and apoptosis.[53] Additionally, triterpenes, such as lupeol acetate, were reported to have cardioprotective effects by inhibiting lipid abnormalities and abnormal biochemical changes induced in MI in addition to anti-inflammatory actions.[54,55]

Moreover, anthocyanins, cyanidin, and their derivatives possess cardioprotective activity due to their antioxidant, anti-inflammatory actions, and inhibiting endothelial dysfunction and NO production.[56] Chlorogenic acid and quercetin-*O*-glucoside also had a cardioprotective,[57,58] and anti-depressant actions.[59,60]

4. Conclusions

We demonstrated that *M. macroura* DCM-S and DCM-L fractions harbor cardioprotective and antidepressive properties against ISO-induced post-MI depression as they persuade cardioprotection by decreasing myocardial enzymes and safeguarding the cardiac muscle histology. Likewise, they maintain emotional stability by boosting serotonin, dopamine, GABA, and ATP brain levels. Also, they restore the redox status of the brain by increasing SOD and GSH levels and protecting its architecture. Further studies in humans are necessitated to examine the clinical application of such observations, such as screening the ligands that support pharmacokinetics, as well as, *in vivo* dose determination, safety, and efficacy studies. The biological results may be attributed to the metabolite profile identified in DCM-L and DCM-S fractions and analyzed using UPLC-ESI-MS/MS.

Conflicts of interest

The authors declared no conflict of interest.

References

1 D. K. Arnett, R. S. Blumenthal, M. A. Albert, A. B. Buroker, Z. D. Goldberger, E. J. Hahn, C. D. Himmelfarb, A. Khera, D. Lloyd-Jones, J. W. McEvoy, E. D. Michos, M. D. Miedema, D. Muñoz, S. C. Smith, S. S. Virani, K. A. Williams, J. Yeboah and B. Ziaeian, ACC/AHA Guideline on the Primary Prevention of Cardiovascular Disease: A Report of the American College of Cardiology/ American Heart Association Task Force on Clinical Practice Guidelines, *Circulation*, 2012, **140**, 596–646.

2 A. Meijer, H. J. Conradi, E. H. Bos, M. Anselmino, R. M. Carney, J. Denollet, F. Doyle, K. E. Freedland, S. L. Grace, S. H. Hosseini, D. A. Lane, L. Pilote, K. Parakh, C. Rafanelli, H. Sato, R. P. Steeds, C. Welin and P. de Jonge, Adjusted prognostic association of depression following myocardial infarction with mortality and cardiovascular events: individual patient data meta-analysis, *Br. J. Psychiatry*, 2013, **203**, 90–102.

3 F. Doyle, H. M. McGee, R. M. Conroy and M. Delaney, What predicts depression in cardiac patients: Sociodemographic

factors, disease severity or theoretical vulnerabilities?, *Psychol. Health*, 2011, **26**, 619–634.

4 S. J. Dai, Z. B. Ma, Y. Wu, R. Y. Chen, D. Q. Yu and F. -J. Guangsangons, Antioxidant and anti-inflammatory Diels–Alder type adducts, from *Morus macroura Miq*, *Phytochemistry*, 2004, **65**, 3135–3141.

5 Y. Wang, L. Xu, W. Gao, L. Niu, C. Huang, P. Yang and X. Hu, Isoprenylated Phenolic Compounds from Morus macroura as Potent Tyrosinase Inhibitors, *Planta Med.*, 2017, **84**, 336–343.

6 P. M. Boarescu, I. Chirilă, A. E. Bulboacă, I. C. Bocșan, R. M. Pop, D. Gheban and S. D. Bolboacă, Effects of Curcumin Nanoparticles in Isoproterenol-Induced Myocardial Infarction, *Oxid. Med. Cell. Longevity*, 2019, **2019**, e7847142.

7 C. Zhu, W. Li, X. Wang, J. Xue, L. Zhao, Y. Song, T. Zhou and M. Zhang, Phloroglucinol averts isoprenaline hydrochloride induced myocardial infarction in rats, *Drug Dev. Res.*, 2019, **80**, 453–460.

8 N. Sun, Y. Mei, Z. Hu, W. Xing, K. Lv, N. Hu, T. Zhang and D. Wang, Ghrelin attenuates depressive-like behavior, heart failure, and neuroinflammation in postmyocardial infarction rat model, *Eur. J. Pharmacol.*, 2021, **901**, 174096.

9 H. Wang, M. Ahmad, R. Jadayel, F. Najjar, D. Lagace and F. Leenen, Inhibition of inflammation by minocycline improves heart failure and depression-like behaviour in rats after myocardial infarction, *PloS one*, 2019, **14**, e0217437.

10 Y. Hu, X. Liu, T. Zhang, C. Chen, X. Dong, Y. Can and P. Liu, Behavioral and Biochemical Effects of KXS on Postmyocardial Infarction Depression, *Front. Pharmacol.*, 2020, **11**, 561817.

11 D. Hamdan, R. A. El-Shiekh, M. El-Sayed, H. M. Khalil, M. Mousa, A. Al-Gendy and A. El-Shazly, Phytochemical characterization and anti-inflammatory potential of Egyptian *Murcott mandarin* cultivar waste (stem, leaves and peel), *Food Funct.*, 2020, **11**, 8214–8236.

12 S. Ali, S. Mohamed, N. Rozalei, Y. Boon and S. Zainalabidin, Anti-fibrotic Actions of Roselle Extract in Rat Model of Myocardial Infarction, *Cardiovasc. Toxicol.*, 2019, **19**, 72–81.

13 H. M. A. Khalil, H. A. Eliwa, R. A. El-Shiekh, A. K. Al-Mokaddem, M. Hassan, A. M. Tawfek and W. H. El-Maadawy, Ashwagandha (*Withania somnifera*) root extract attenuates hepatic and cognitive deficits in thioacetamide-induced rat model of hepatic encephalopathy *via* induction of Nrf2/HO-1 and mitigation of NF-kB/MAPK signaling pathways, *J. Ethnopharmacol.*, 2021, **277**, 114141.

14 S. M. Zaki, G. H. A. Hussein, H. A. M. Khalil and W. A. A. Algaleel, Febuxostat ameliorates methotrexate-induced lung damage, *Folia Morphol.*, 2020, **80**, 392–402.

15 D. A. Slattery and J. F. Cryan, Using the rat forced swim test to assess antidepressant-like activity in rodents, *Nat. Protoc.*, 2012, **7**, 1009–1014.

16 T. Teerlink, M. Hennekes, J. Bussemaker and J. Groeneveld, Simultaneous Determination of Creatine Compounds and Adenine Nucleotides in Myocardial Tissue by High-Performance Liquid Chromatography, *Anal. Biochem.*, 1993, **214**, 278–283.

17 P. Pagel, J. Blome and H. U. Wolf, High-performance liquid chromatographic separation and measurement of various biogenic compounds possibly involved in the pathomechanism of Parkinson's disease, *J. Chromatogr. B Biomed. Appl.*, 2000, **746**, 297–304.

18 J. D. Bancroft, and M. Gamble, *Theory and practice of histology techniques*, Churchill Livingstone Elsevier Lond., 2008, pp. 83–134.

19 C. Atkinson, S. He, K. Morris, F. Qiao, S. Casey, M. Goddard and S. Tomlinson, Targeted Complement Inhibitors Protect against Posttransplant Cardiac Ischemia and Reperfusion Injury and Reveal an Important Role for the Alternative Pathway of Complement Activation, *J. Immunol. Res.*, 2010, **185**, 7007–7013.

20 H. C. Huang, C. C. Liaw, H. L. Yang, Y. C. Hseu, H. T. Kuo, Y. C. Tsai and Y. H. Kuo, Lanostane triterpenoids and sterols from *Antrodia camphorate*, *Phytochemistry*, 2012, **84**, 177–183.

21 A. S. Kipkemei, Isolation of stigmasterol, α-amyrin acetate and lupeol acetate from *Tabernaemontana Stapfiana* Britten, *Int. J. Sci. Eng. Res.*, 2017, **8**, 1331–1335.

22 H. Li, Z. Ma, Y. Zhai, C. Lv, P. Yuan, F. Zhu, L. Wei, Q. Li and X. Qi, Trimetazidine Ameliorates Myocardial Metabolic Remodeling in Isoproterenol-Induced Rats Through Regulating Ketone Body Metabolism *via* Activating AMPK and PPAR α, *Front. Pharmacol.*, 2020, **11**, 1255.

23 K. Mnafgui, R. Hajji, F. Derbali, A. Gammoudi, G. Khabbabi, H. Ellefi, N. Allouche, A. Kadri and N. Gharsallah, Anti-inflammatory, Antithrombotic and Cardiac Remodeling Preventive Effects of Eugenol in Isoproterenol-Induced Myocardial Infarction in Wistar Rat, *Cardiovasc. Toxicol.*, 2016, **16**, 336–344.

24 M. Raish, A. Ahmad, M. Ansari, K. Alkharfy, A. Ahad, A. Khan, N. Ali and M. Ganaie, Beetroot juice alleviates isoproterenol-induced myocardial damage by reducing oxidative stress, inflammation, and apoptosis in rats, *Biotech.*, 2019, **9**, 147.

25 D. Mozaffarian, H. Cao, I. B. King, R. N. Lemaitre, X. Song, D. S. Siscovick and G. S. Hotamisligil, Trans-palmitoleic acid, metabolic risk factors, and new-onset diabetes in US adults: a cohort study, *Ann. Intern. Med.*, 2010, **153**, 790–799.

26 P. Akila, L. Asaikumar and L. Vennila, Chlorogenic acid ameliorates isoproterenol-induced myocardial injury in rats by stabilizing mitochondrial and lysosomal enzymes, *Biomed. Pharmacother.*, 2017, **85**, 582–591.

27 M. Sumitra, P. Manikandan, D. A. Kumar, N. Arutselvan, K. Balakrishna, B. M. Manohar and R. Puvanakrishnan, Experimental myocardial necrosis in rats: role of arjunolic acid on platelet aggregation, coagulation and antioxidant status, *Mol. Cell. Biochem.*, 2001, **224**, 135–142.

28 R. Zhou, P. Ma, A. Xiong, Y. Xu, Y. Wang and Q. Xu, Protective effects of low-dose rosuvastatin on isoproterenol-induced chronic heart failure in rats by regulation of DDAH-ADMA-NO pathway, *Cardiovasc. Ther.*, 2017, **35**, 12241.

29 S. N. Fathima and S. V. Murthy, Cardioprotective effects to chronic administration of *Rosa damascena* petals in isoproterenol induced myocardial infarction: biochemical, histopathological and ultrastructural studies, *Biomed. Pharmacol. J.*, 2019, **12**, 1155–1166.

30 M. Li, X. Li and L. Yang, Cardioprotective effects of garcinol following myocardial infarction in rats with isoproterenol-induced heart failure, *AMB Express*, 2020, **10**, 1–7.

31 K. Mal, I. D. Awan, J. Ram and F. Shaukat, Depression and Anxiety as a Risk Factor for Myocardial Infarction, *Cureus*, 2019, **11**, e6064.

32 K. R. Lezak, G. Missig and W. A. Carlezon Jr, Behavioral methods to study anxiety in rodents, *Dialogues Clin. Neurosci.*, 2017, **19**, 181–191.

33 A. K. Kraeuter, P. C. Guest and Z. Sarnyai, The Forced Swim Test for Depression-Like Behavior in Rodents, *Methods Mol. Biol.*, 2019, **1916**, 75–80.

34 A. Frey, S. Popp, A. Post, S. Langer, M. Lehmann, U. Hofmann, A. L. Sirén, L. Hommers, A. Schmitt, T. Strekalova, G. Ertl, K. P. Lesch and S. Frantz, Experimental heart failure causes depression-like behavior together with differential regulation of inflammatory and structural genes in the brain, *Front. Behav. Neurosci.*, 2014, **8**, 376.

35 N. Sun, Y. Mei, Z. Hu, W. Xing, K. Lv, N. Hu, T. Zhang and D. Wang, Ghrelin attenuates depressive-like behavior, heart failure, and neuroinflammation in postmyocardial infarction rat model, *Eur. J. Pharmacol.*, 2021, **901**, 174096.

36 M. Williams, Platelets and depression in cardiovascular disease: A brief review of the current literature, *World J. Psychiatry*, 2012, **2**, 114–123.

37 M. Naoi, W. Maruyama and M. Shamoto-Nagai, Type A monoamine oxidase and serotonin are coordinately involved in depressive disorders: from neurotransmitter imbalance to impaired neurogenesis, *J. Neural Transm.*, 2018, **125**, 53–66.

38 H. G. Ruhé, N. S. Mason and A. H. Schene, A Mood is indirectly related to serotonin, norepinephrine and dopamine levels in humans: a meta-analysis of monoamine depletion studies, *Mol. Psychiatry*, 2007, **12**, 331–359.

39 H. Zhang, Z. Ma, X. Luo and X. Li, Effects of mulberry fruit (*Morusalba* L.) consumption on health outcomes: A mini-review, *Antioxidants*, 2018, **7**, 69.

40 C. Fee, M. Banasr and E. Sibille, Somatostatin-Positive Gamma-Aminobutyric Acid Interneuron Deficits in Depression: Cortical Microcircuit and Therapeutic Perspectives, *Biol. Psychiatry*, 2017, **82**, 549–559.

41 C. G. Abdallah, L. Jiang, H. M. De Feyter, M. Fasula, J. H. Krystal, D. L. Rothman, G. F. Mason and G. Sanacora, Glutamate Metabolism in Major Depressive Disorder, *Am. J. Psychiatry.*, 2014, **171**, 1320–1327.

42 A. Moretti, A. Gorini and R. F. Villa, Affective disorders, anti-depressant drugs and brain metabolism, *Mol. Psychiatry*, 2003, **8**, 773–785.

43 M. J. Devine and J. T. Kittler, Mitochondria at the neuronal presynapse in health and disease, *Nat. Rev. Neurosci.*, 2018, **19**, 63–80.

44 A. Karabatsiakis and C. Schönfeldt-Lecuona, Depression, mitochondrial bioenergetics, and electroconvulsive therapy: a new approach towards personalized medicine in psychiatric treatment - a short review and current perspective, *Transl. Psychiatry*, 2020, **10**, 1–9.

45 D. Martins-de-Souza, P. C. Guest, L. W. Harris, N. Vanattou-Saifoudine, M. J. Webster, H. Rahmoune and S. Bahn, Identification of proteomic signatures associated with depression and psychotic depression in post-mortem brains from major depression patients, *Transl. Psychiatry*, 2012, **2**, 87.

46 M. Maes, P. Galecki, Y. S. Chang and M. Berk, A review on the oxidative and nitrosative stress (O&NS) pathways in major depression and their possible contribution to the (neuro) degenerative processes in that illness, *Prog. Neuropsychopharmacol. Biol. Psychiatry*, 2011, **35**, 676–692.

47 Y. Kurhe, M. Radhakrishnan, D. Gupta and T. Devadoss, QCM-4 a novel 5-HT3 antagonist attenuates the behavioral and biochemical alterations on chronic unpredictable mild stress model of depression in Swiss albino mice, *J. Pharm. Pharmacol.*, 2014, **66**, 122–132.

48 D. Arnone, S. McKie, R. Elliott, G. Juhasz, E. J. Thomas, D. Downey, S. Williams, J. F. Deakin and I. M. Anderson, State-dependent changes in hippocampal grey matter in depression, *Mol. Psychiatry*, 2013, **18**, 1265–1272.

49 M. S. Butt, A. Nazir, M. T. Sultan and K. Schroën, *Morus alba* L. nature's functional tonic, *Trends Food Sci. Technol.*, 2008, **19**, 505–512.

50 K. Razavi-Azarkhiavi, M. Iranshahy, A. Sahebkar, K. Shirani and G. Karimi, The Protective Role of Phenolic Compounds Against Doxorubicin-induced Cardiotoxicity : A Comprehensive Review, *Nutr. Cancer*, 2016, **68**, 892–917.

51 G. Grosso, A. Pajak, S. Marventano, S. Castellano, F. Galvano, C. Bucolo, F. Drago and F. Caraci, Role of omega-3 fatty acids in the treatment of depressive disorders: a comprehensive meta-analysis of randomized clinical trials, *PLoS One*, 2014, **9**, e96905.

52 L. Carnevali, F. Vacondio, S. Rossi, S. Callegari, E. Macchi, G. Spadoni, A. Bedini, S. Rivara, M. Mor and A. Sgoifo, Antidepressant-like activity and cardioprotective effects of fatty acid amide hydrolase inhibitor URB694 in socially stressed Wistar Kyoto rats, *Eur. Neuropsychopharmacol.*, 2015, **25**, 2157–2169.

53 F. Lin, L. Xu, M. Huang, B. Deng, W. Zhang, Z. Zeng and S. Yinzhi, β-Sitosterol Protects against Myocardial Ischemia/Reperfusion Injury *via* Targeting PPARγ/NF-κB Signalling, *Evidence-Based Complementary Altern. Med.*, 2020, **28**, 2679409.

54 V. Sudhahar, S. A. Kumar, P. T. Sudharsan and P. Varalakshmi, Protective effect of lupeol and its ester on cardiac abnormalities in experimental hypercholesterolemia, *Curr. Vasc. Pharmacol.*, 2007, **46**, 412–418.

55 S. Saha, E. Profumo, A. R. Togna, R. Riganò, L. Saso and B. Buttari, Lupeol Counteracts the Proinflammatory Signalling Triggered in Macrophages by 7-Keto-Cholesterol:

New Perspectives in the Therapy of Atherosclerosis, *Oxid. Med. Cell. Longevity*, 2020, **2020**, 1232816.

56 J. Liu, H. Zhou, L. Song, Z. Yang, M. Qiu, J. Wang and S. Shi, Anthocyanins: Promising Natural Products with Diverse Pharmacological Activities, *Molecules*, 2021, **26**, 3807.

57 M. Li, Y. Jiang, W. Jing, B. Sun, C. Miao and L. Ren, Quercetin provides greater cardioprotective effect than its glycoside derivative rutin on isoproterenol-induced cardiac fibrosis in the rat, *Can. J. Physiol. Pharmacol.*, 2013, **91**, 951–959.

58 O. M. Agunloye, G. Oboh, A. O. Ademiluyi, A. O. Ademosun, A. A. Akindahunsi, A. A. Oyagbemi, T. O. Omobowale, T. O. Ajibade and A. A. Adedapo, Cardio-protective and antioxidant properties of caffeic acid and chlorogenic acid:

Mechanistic role of angiotensin converting enzyme, cholinesterase and arginase activities in cyclosporine induced hypertensive rats, *Biomed. Pharmacother.*, 2019, **109**, 450–458.

59 S. Park, Y. Sim, P. Han, J. Jin-Koo Lee and H. Suh, Antidepressant-like effect of chlorogenic acid isolated from *Artemisia capillaris* Thunb, *Anim. Cells Syst.*, 2010, **4**, 253–259.

60 V. Singh, G. Chauhan and R. Shri, Anti-depressant like effects of quercetin 4'-O-glucoside from Allium cepa *via* regulation of brain oxidative stress and monoamine levels in mice subjected to unpredictable chronic mild stress, *Nutr. Neurosci.*, 2021, **2**, 35–44.